

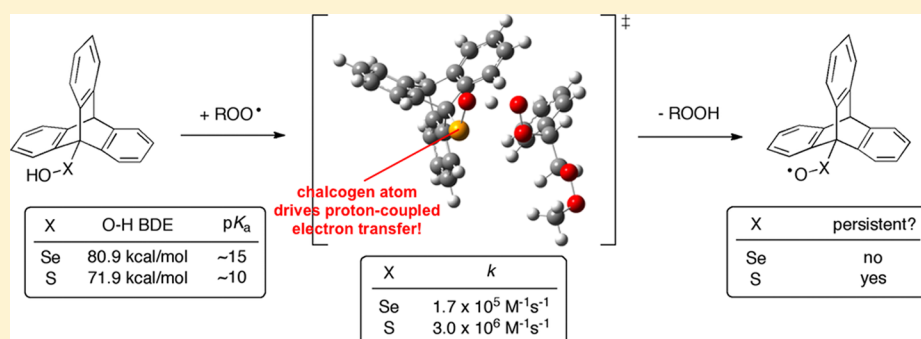
Redox Chemistry of Selenenic Acids and the Insight It Brings on Transition State Geometry in the Reactions of Peroxyl Radicals

Zosia Zielinski,[†] Nathalie Presseau,[†] Riccardo Amorati,[‡] Luca Valgimigli,^{*,‡} and Derek A. Pratt^{*,†}

[†]Department of Chemistry, University of Ottawa, Ottawa, Ontario K1N 6N5, Canada

[‡]Department of Chemistry "G. Ciamician", University of Bologna, I-40126 Bologna, Italy

S Supporting Information

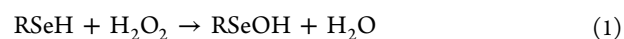


ABSTRACT: The redox chemistry of selenenic acids has been explored for the first time using a persistent selenenic acid, 9-triptyceneselenenic acid (RSeOH), and the results have been compared with those we recently obtained with its lighter chalcogen analogue, 9-triptycenesulfenic acid (RSOH). Specifically, the selenenyl radical was characterized by EPR spectroscopy and equilibrated with a phenoxyl radical of known stability in order to determine the O–H bond dissociation enthalpy of RSeOH (80.9 ± 0.8 kcal/mol): ca. 9 kcal/mol stronger than in RSOH. Kinetic measurements of the reactions of RSeOH with peroxy radicals demonstrate that it readily undergoes H-atom transfer reactions (e.g., $k = 1.7 \times 10^5 \text{ M}^{-1} \text{ s}^{-1}$ in PhCl), which are subject to kinetic solvent effects and kinetic isotope effects similar to RSOH and other good H-atom donors. Interestingly, the rate constants for these reactions are only 18- and 5-fold smaller than those measured for RSOH in PhCl and CH₃CN, respectively, despite being 9 kcal/mol less exothermic for RSeOH. IR spectroscopic studies demonstrate that RSeOH is less H-bond acidic than RSOH, accounting for these solvent effects and enabling estimates of the pK_as in RSeOH and RSOH of ca. 15 and 10, respectively. Calculations suggest that the TS structures for these reactions have significant charge transfer between the chalcogen atom and the internal oxygen atom of the peroxy radical, which is nominally better for the more polarizable selenenic acid. The higher than expected reactivity of RSeOH toward peroxy radicals is the strongest experimental evidence to date for charge transfer/secondary orbital interactions in the reactions of peroxy radicals with good H-atom donors.

INTRODUCTION

Selenenic acids (RSeOH) are the selenium analogues of sulfenic acids (RSOH), both being the heavier (valence) isoelectronic cousins to the more commonly encountered hydroperoxides (ROOH). Selenenic acids are believed to be transient intermediates in a number of redox reactions involving organoselenium compounds, inferred largely from the analogous chemistry exhibited by sulfenic acids derived from organosulfur compounds.^{1,2} The two most important reactions that lead to selenenic acids are the oxidation of a selenol (e.g., with H₂O₂ as in eq 1), first demonstrated directly in 2001,³ and syn elimination from a selenoxide (e.g., eq 2), a common synthetic transformation for late-stage introduction of an alkene.^{4–6} The former reaction is believed to be key to the essential antioxidant enzyme glutathione peroxidase,^{7,8} whose active site selenocysteine residue is responsible for the reduction of hydroperoxides and H₂O₂ to alcohols and water, respectively, prompting the widespread pursuit of small-

molecule mimics for therapeutic and/or chemopreventive purposes against disease wherein oxidative stress has been implicated.⁹



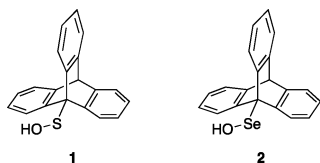
Despite their prominence in these (and other¹) roles, the properties of selenenic acids have been elusive, owing to the ease with which they self-condense, disproportionate, and/or oxidize. While the synthesis of isolable selenenic acids has been pursued for some time,¹⁰ with a handful of examples of sterically hindered areneselenenic acids being reported,^{3,11} as well as a single alkaneselenenic acid,¹² essentially no investigation of their physicochemical properties has accom-

Received: November 18, 2013

Published: January 2, 2014

panied them. Of particular interest are their redox characteristics, which are expected to figure prominently in their chemistry.

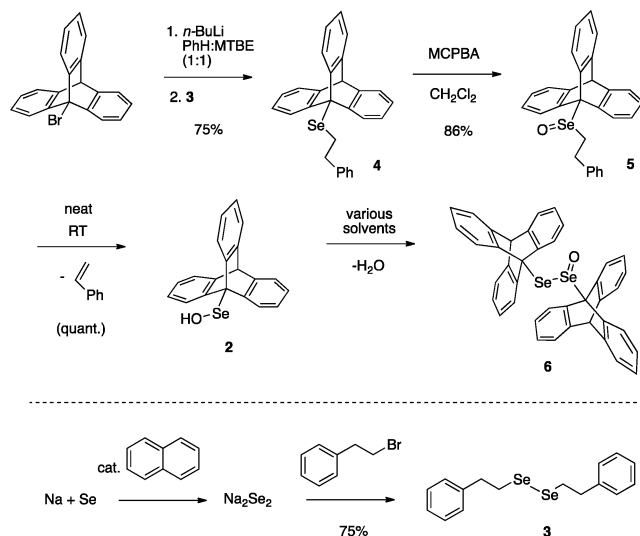
We recently reported the results of detailed studies on the redox chemistry of a persistent sulfenic acid, 9-triptycenesulfenic acid (**1**), in order to provide a thermodynamic¹³ and kinetic¹⁴ rationale for the involvement of sulfenic acids in the radical-trapping antioxidant activity of natural product organosulfur compounds, such as the garlic-derived allicin¹⁵ and anamu-derived petivericin,¹⁶ as well as sulfenic acid mediated processes, including cysteine-mediated redox cell signaling.¹⁷ In an effort to shed light on the redox chemistry of selenenic acids and provide a basis for a direct comparison of their electronic properties with those of sulfenic acids (and hydroperoxides), we report here the results of corresponding studies on the selenium analogue of **1**: 9-triptyceneselenenic acid (**2**).¹² The studies described herein provide important fundamental insights into the thermodynamics and kinetics of radical reactions of selenenic acids, in particular, and provide a unique perspective on the importance of transition state geometry in formal H-atom transfer reactions to autoxidation chain-carrying peroxy radicals, in general.



RESULTS AND DISCUSSION

9-Triptyceneselenenic acid (**2**)¹² was prepared as shown in Scheme 1. Briefly, 9-bromotriptycene was subjected to

Scheme 1. Synthesis of 9-Triptyceneselenenic Acid **2** and Its Condensation to the Corresponding Selenoseleninate **6**



lithium–halogen exchange, and the resultant organolithium was quenched with bis(phenethyl) diselenide (**3**), which was prepared from phenethyl bromide as suggested by Thompson and Boudjouk.³⁶ The resultant selenide **4** was then oxidized with MCPBA to yield the selenoxide **5**, which underwent Cope-type elimination at room temperature to give **2**. The successful isolation of **2** required the solid-state decomposition of the precursor selenoxide under high vacuum over a 2 week period

to minimize the self-condensation of **2** to give the corresponding selenoseleninate **6**. As such, solutions of **2** were prepared immediately prior to use in the experiments reported below.

A deoxygenated solution of the selenenic acid in benzene was photolyzed in the presence of 10% (by volume) di-*tert*-butyl peroxide in the cavity of an X-band EPR spectrometer, affording the noisy spectrum shown in Figure 1. The field

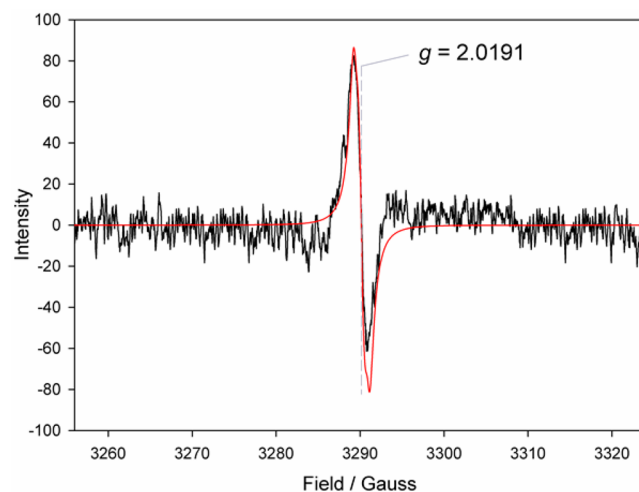


Figure 1. EPR spectrum of the selenenyl radical generated from continuous photolysis of a solution of **2** in benzene containing 10% di-*tert*-butyl peroxide. The simulated spectrum is shown in red.

center of the broad singlet (2.4 G line width) is $g = 2.0191$, consistent with an oxygen-centered radical with spin delocalization onto a heavier atom and slightly larger than that of the corresponding sulfinyl radical derived from the analogous sulfenic acid **1**, for which we had measured $g = 2.0114$.¹³ Continuous photolysis was necessary as the resultant selenenyl radical decayed on the time scale of the acquisition, yielding only the weak signal shown which prevented resolution of the coupling with ⁷⁷Se (which has a nuclear spin of $I = +1/2$ and is 7.6% at natural abundance).

While the selenenyl radical was not particularly persistent, we hoped that its rapid equilibration with a compound of known O–H BDE^{13,18,19} would allow the determination of the O–H BDE of a selenenic acid for the first time. To provide guidance on which compound to use in the equilibration experiment, we carried out computations on a model selenenic acid (*t*-BuSeOH), for which CBS-QB3²⁰ calculations predicted an O–H BDE of 81.2 kcal/mol. On the basis of this result we chose 2,4,6-tri-*tert*-butylphenol (TTBP) as the reference compound for the equilibration experiment, as it has an O–H BDE of 80.1 kcal/mol¹⁹ and yields a persistent phenoxyl radical upon H-atom abstraction. Gratifyingly, continuous photolysis of mixtures of selenenic acid and TTBP in benzene containing 10% di-*tert*-butyl peroxide (by volume) afforded spectra showing both the selenenyl and phenoxyl radicals (cf. Figure 2). Equilibrium constants of $K = 4.0 \pm 2.1$ were obtained from simulation of the spectra, which afford $\Delta H = 0.8 \pm 0.4$ kcal/mol assuming a negligible entropy change for the formal H atom transfer process and therefore an O–H BDE of 80.9 ± 0.8 kcal/mol for **2**.

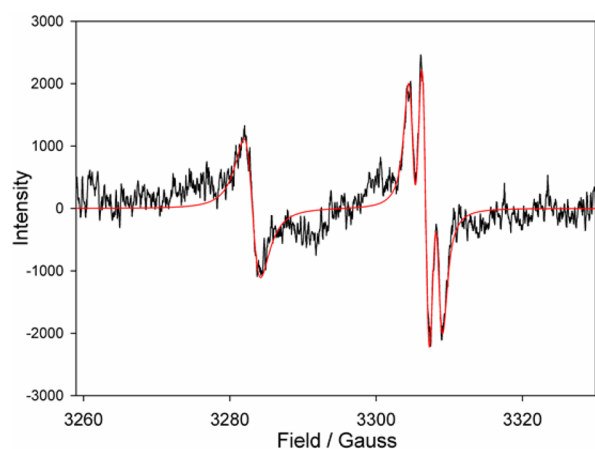
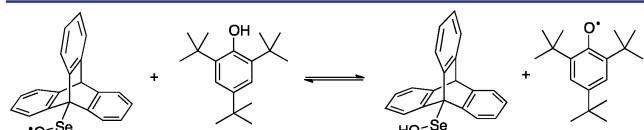


Figure 2. Representative EPR spectrum obtained from continuous photolysis of a 1:1 mixture of **2** and 2,4,6-tri-*tert*-butylphenol in benzene containing 10% di-*tert*-butyl peroxide. The simulated spectrum for a 4:1 mixture of the 2,4,6-tri-*tert*-butylphenoxy and selenenyl radicals is shown in red.



The increased strength of the O–H bond in the selenenic acid in comparison to the sulfenic acid (71.9 ± 0.3 kcal/mol, also measured by the radical equilibration EPR approach; for comparison CBS-QB3 predicts an O–H BDE of 68.6 kcal/mol in *t*-BuSOH)^{13,42} can be rationalized by the longer Se–O bond in the selenenyl radical as compared to the S–O bond in the sulfenyl radical. The calculated minimum energy structures of the *tert*-butyl selenenyl and sulfenyl radicals from the CBS-QB3 calculations are shown in Figure 3, wherein the Se–O and S–O

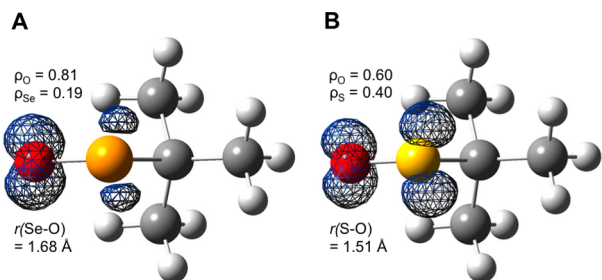


Figure 3. Calculated structures and spin density distributions in *t*-BuSeO• (A) and *t*-BuSO• (B).

bond distances are 1.68 and 1.51 Å, respectively. The associated spin delocalization in the selenenyl radical is predicted to be ca. 20% on the selenium atom and 80% on the oxygen atom as compared to ca. 40% on the sulfur atom and 60% on the oxygen atom in the sulfenyl radical.⁴³

It is of interest to compare the O–H BDE in a selenenic acid to the Se–H BDE in a selenol—often its direct precursor in redox reactions, such as in the catalytic cycle of glutathione peroxidase (as in eq 1). Since, to the best of our knowledge, no experimental value is available for the Se–H BDE of an alkaneselenol (the Se–H BDEs for HSeH and PhSeH are reported to be 79.0 ± 0.2 ²¹ and 78 ± 4 kcal/mol,²² respectively), we calculated it for *t*-BuSeH using CBS-QB3 to allow for direct comparison to the foregoing calculations on *t*-

BuSeOH. These calculations reveal that the O–H bond in *t*-BuSeOH (81.2 kcal/mol) is *slightly stronger* than the Se–H bond in *t*-BuSeH (78.9 kcal/mol). This result is particularly interesting because the trend is completely different from that observed for the lighter chalcogen: the O–H bond in *t*-BuSOH (68.6 kcal/mol) is *much weaker* than the S–H bond in *t*-BuSH (87.6 kcal/mol).²³ This fundamentally different trend—which is rooted in the very high stability of the sulfinyl radical¹³—underscores the need for caution when rationalizing the reactivity of selenium-containing compounds simply on the basis of their similarity to sulfur-containing compounds.

Electrochemical experiments also suggest that selenenic acids are more difficult to oxidize than sulfenic acids. Cyclic voltammograms, which were irreversible at scan rates ranging from 1 to 1000 mV/s, consistently showed anodic (oxidation) peaks at potentials that were ca. 200 mV more oxidizing than for the sulfenic acid under identical conditions (representative voltammograms are given in the Supporting Information). Attempts to obtain reversible voltammograms by addition of acid to suppress deprotonation of the resultant radical cation (and subsequent rapid reactions of the selenenyl radical; vide supra) led to no observable signal in the potential window, presumably due to acid catalysis of the self-condensation of the selenenic acid to yield the selenoseleninate **6**. Likewise, addition of base to yield the selenenate anion in the hopes of obtaining a reversible RSeO•/RSeO[−] couple also led to no observable signal in the potential window, again due to base-catalyzed formation of the selenoseleninate **6**.

The H-atom transfer reactivity of the selenenic acid was probed in studies of the kinetics of its reactions with peroxy radicals, the results of which could be compared to the results of analogous experiments we previously carried out on the corresponding sulfenic acid.¹⁴ These measurements were made using the well-established inhibited autoxidation of styrene approach, using O₂ consumption to monitor reaction progress (cf. Figure 4), from which rate constants could be determined for the formal H-atom transfer (k_{inh}) from the initial rates (Table 1).²⁴ In chlorobenzene, a rate constant of $(1.7 \pm 0.3) \times 10^5 \text{ M}^{-1} \text{ s}^{-1}$ was obtained, indicating that selenenic acids are indeed very reactive in H-atom transfer reactions. For comparison, the analogous sulfenic acid reacts with a rate

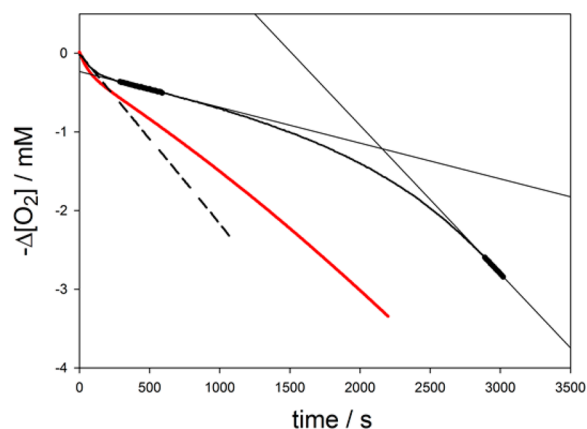


Figure 4. Oxygen consumption during the autoxidation of styrene (50% by volume) initiated by AIBN (0.05 M) at 303 K without inhibitor (dashed line) or in the presence of **2** (7.6 μM) in PhCl + 0.5% CH₃OH (black line) or PhCl + 0.5% CH₃OD (red line). The resultant $k_{\text{H}}/k_{\text{D}}$ value is 2.9.

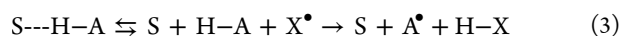
Table 1. Rate Constants (k_{inh}) for the Reactions of Selenenic Acid **2** with Peroxyl Radicals at 303 K^a

conditions	k_{inh} ($\text{M}^{-1} \text{s}^{-1}$)	
	2	1 ^c
styrene/PhCl	$(1.7 \pm 0.3) \times 10^5$	$(3.0 \pm 0.3) \times 10^6$
styrene/ CH_3CN	$(3.5 \pm 0.4) \times 10^4$	$(1.6 \pm 0.3) \times 10^5$
styrene/ $\text{CH}_3\text{CN}/\text{H}_2\text{O}^b$	$(3.4 \pm 0.3) \times 10^4$	$(1.1 \pm 0.2) \times 10^5$
styrene/ $\text{CH}_3\text{CN}/\text{D}_2\text{O}^b$	$(5.1 \pm 0.6) \times 10^3$	$(1.8 \pm 0.2) \times 10^4$
$k_{\text{H}}/k_{\text{D}}$	6.7 ± 0.9	6.1 ± 0.4

^aLiterature data for the reactions of sulfenic acid **1** obtained under the same conditions are presented for comparison. ^b H_2O or D_2O added in 1% v/v. ^cTaken from ref 13.

constant of $(3.0 \pm 0.3) \times 10^6 \text{ M}^{-1} \text{ s}^{-1}$ under identical conditions,¹⁴ a reactivity that is identical with that of α -tocopherol, nature's premier lipid-soluble radical-trapping antioxidant, under equivalent conditions.²⁴ A kinetic solvent effect diminishes the reactivity of **2** by a factor of 4.9 on moving from chlorobenzene to acetonitrile, in comparison to a factor of 19 for **1**. As in our previous studies with sulfenic acid **1**,¹⁴ a large primary deuterium kinetic isotope effect was determined for the reaction of **2** with peroxy radicals, consistent with a formal H-atom transfer mechanism.

Ingold has shown that the rates of H-atom transfer reactions vary in different solvents (S) according to a model that assumes the H-atom donor (H-A) is unreactive when its labile H-atom is involved in an H-bond with the solvent.^{25,26} As a result, the kinetics can be accurately described only using a model that involves a predissociation of this H-bonded complex:



Ingold went on to show that the solvent effects could be quantitated using an empirical linear free energy relationship based on the H-bond donating strength of the H-atom donor (α_2^{H}) and the H-bond accepting strength of the solvent (β_2^{H}):

$$\log k^{\text{S}} = -8.3\alpha_2^{\text{H}}\beta_2^{\text{H}} + \log k^0 \quad (4)$$

As such, the larger kinetic solvent effect on the reaction of the sulfenic acid in comparison to the selenenic acid implies that the former is a better H-bond donor than the latter.

Indeed, FT-IR spectra of **1** and **2** obtained in the non-H-bond accepting solvent CCl_4 in the presence of increasing amounts of acetonitrile reveal trends that are consistent with the observed kinetic solvent effects. From these spectra, the equilibrium constants corresponding to H-bond formation between **1** or **2** and acetonitrile can be derived from the integration of the peak corresponding to the free O–H stretch as a function of acetonitrile concentration (vide infra) to give 2.78 ± 0.45 and $0.92 \pm 0.20 \text{ M}^{-1}$, respectively. Using Abraham's equation, these equilibrium constants yield values of α_2^{H} of 0.54 and 0.37 for **1** and **2**, respectively. On the basis of these values of α_2^{H} , we would expect the rate constants for H-atom transfer from **1** and **2** to peroxy radicals to drop 22- and 8-fold on moving from chlorobenzene ($\beta_2^{\text{H}} = 0.09$)²⁷ to acetonitrile ($\beta_2^{\text{H}} = 0.39$),^{27,44} from Ingold's eq 4,²⁵ in excellent agreement with the experimental results of 19 and 4.9, respectively.⁴⁵

It should be pointed out that the values of α_2^{H} derived from the FT-IR measurements also provide some insight into the relative acidities of **1** and **2**. Since the H-bond donating ability generally correlates with the $\text{p}K_{\text{a}}$ of the donor, it can be expected that **1** has a $\text{p}K_{\text{a}}$ similar to that of phenol ($\alpha_2^{\text{H}} = 0.60$,

$\text{p}K_{\text{a}} \approx 10$),¹⁰ while **2** has a $\text{p}K_{\text{a}}$ similar to that of methanol ($\alpha_2^{\text{H}} = 0.37$, $\text{p}K_{\text{a}} \approx 15$).¹⁰ We had previously measured a $\text{p}K_{\text{a}}$ value of 12.5 for **1** in 4/1 $\text{CH}_3\text{CN}/\text{H}_2\text{O}$, which would undoubtedly be slightly lower in water, but attempts to measure the $\text{p}K_{\text{a}}$ of **2** under similar conditions were unsuccessful owing to selenoseleninate formation under the conditions of the potentiometric titration.

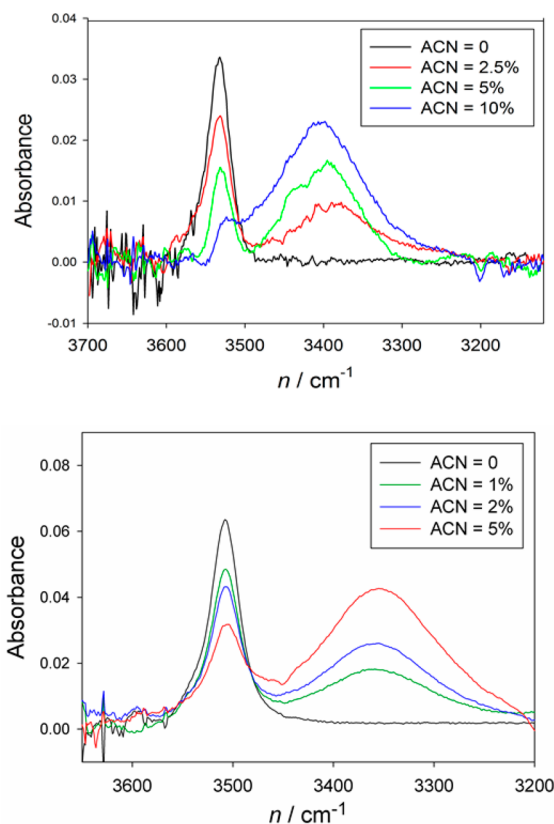


Figure 5. Representative FT-IR spectra of the O–H stretching region of **2** (5 mM, top) and **1** (10 mM, bottom) in CCl_4 containing increasing amounts of acetonitrile as cosolvent.

At first glance, the slower reaction of the selenenic acid with peroxy radicals relative to the sulfenic acid appears fully consistent with the fact that the selenenic acid has a stronger O–H bond. However, Evans–Polanyi relationships between rate constants for the reactions of H-atom donors with peroxy radicals (k_{inh}) and the X–H BDEs of the H-atom donors imply that a much larger reactivity difference should exist between the selenenic and sulfenic acids given the 9 kcal/mol difference in their O–H BDEs. For instance, the Evans–Polanyi correlations in Figure 6 for 4-substituted phenols, 4-substituted 2,6-dimethylphenols, and 4-substituted 2,6-di-*tert*-butylphenols predict differences of 3 orders of magnitude in k_{inh} for an O–H BDE difference of 9 kcal/mol.²⁸ Interestingly, including the data for **1** and **2** in these correlations finds them on the lines of best fit for the 2,6-di-*tert*-butylated phenols and the unsubstituted phenols, respectively. The data for substituted phenols have long been assumed to lie on different lines owing to the differing steric demands on the reactions, which increases the entropy of activation for the more hindered substrates, decreasing the pre-exponential factor for their reactions.²⁸ This implies that the sulfenic and selenenic acids also have different steric requirements. Indeed, the longer C–Se and Se–O bonds

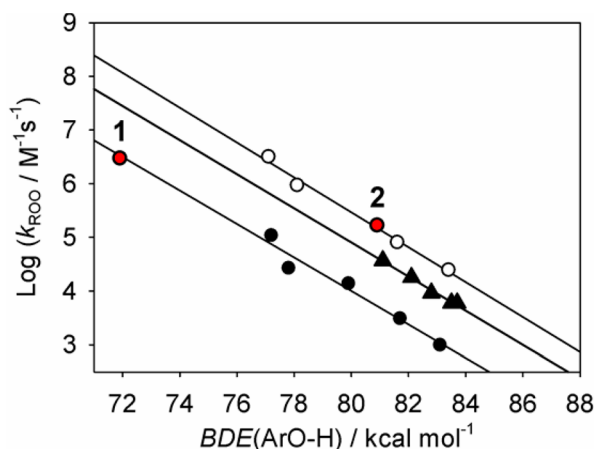


Figure 6. Evans–Polanyi correlations for the reactions of peroxy radicals with 4-substituted phenols (O), 2,6-dimethyl 4-substituted phenols (▲) and 2,6-di-*tert*-butyl 4-substituted phenols (●). Also shown are the corresponding data for **1** and **2**.

in the selenenic acid (1.956 and 1.866 Å, respectively)¹² relative to the C–S and S–O bonds in the sulfenic acid (1.833 and 1.622 Å, respectively)²⁹ should minimize steric interactions between the triptycene moiety and the substituent on the peroxy radical to which the H-atom is being transferred.

To provide insight into the transition state (TS) structures by which these reactions proceed, and the extent to which they are impeded by steric interactions, we again turned to computation. Since TS calculations of reactions of **1** and **2** with peroxy radicals are far too large to be carried out with the high-accuracy CBS-QB3 approach used for the BDE calculations above, we turned to density functional theory using B3LYP and the dispersion-correcting potentials (DCPs) of DiLabio and Torres.³⁰ The calculated minimum energy TS structures are shown in Figure 7, and alongside are the

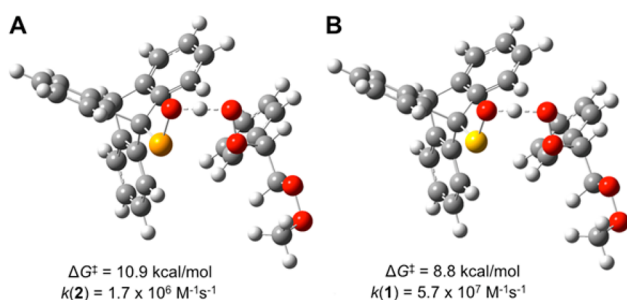


Figure 7. DCP-B3LYP/6-31+G(2d,2p)-calculated transition state structures for the reactions of selenenic acid **2** (A) and sulfenic acid **1** (B) with a styrylperoxy radical (representative of the chain-carrying peroxy radicals in styrene autoxidations).

corresponding thermokinetic parameters. While the calculated rate constants (from transition state theory) are overestimated relative to experiment by roughly 1 order of magnitude,⁴⁶ they are consistent with the experimental results in that they indicate that the selenenic acid **2** reacts more slowly with peroxy radicals than the sulfenic acid **1**. Indeed, the calculated ratio $k(1)/k(2) = 33$ is in very good agreement with the experimental value of $k_{\text{inh}}(1)/k_{\text{inh}}(2) = 18$.

Somewhat surprisingly, the TS structures in Figure 7 feature a syn relationship of the substituents on the oxygen atoms between which the H-atom is being transferred. While previous

CBS-QB3 calculations on less sterically encumbered sulfenic acids (e.g., *t*-BuSOH) and peroxy radicals (MeOO•) indicated that this conformation is preferred by a significant margin over a TS structure wherein the substituents on the oxygen atoms adopt an anti conformation ($\Delta G_{\text{syn}}^{\ddagger} = 10.1$ kcal/mol and $\Delta G_{\text{anti}}^{\ddagger} = 14.9$ kcal/mol, Figure 8B,D),¹⁵ we anticipated that

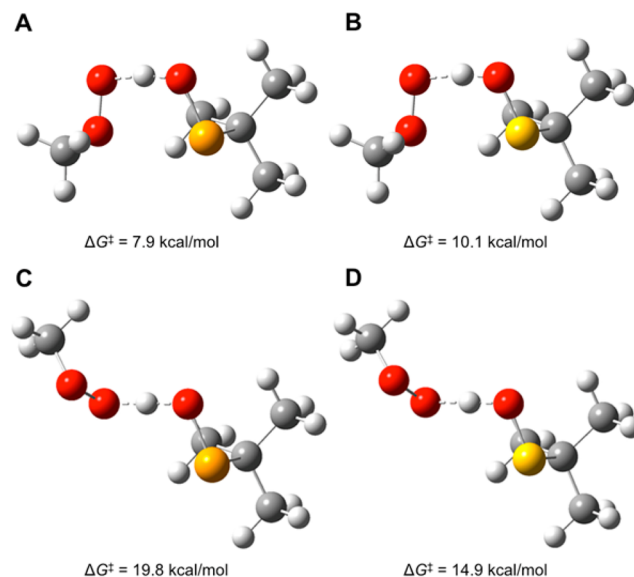


Figure 8. CBS-QB3-calculated syn (A, B) and anti (C, D) transition state structures for the reactions of *t*-BuSeOH (A, C) and *t*-BuSOH (B, D) with a model alkylperoxy radical (MeOO•).

the larger substituents would alter this preference.¹⁴ In order to provide a corresponding unhindered comparison for the selenenic acid, we carried out CBS-QB3 calculations on the reaction of *t*-BuSeOH and MeOO•. Indeed, the same geometric preference is predicted for this reaction (Figure 8A,C), with the syn TS being preferred by an even greater margin over the anti TS ($\Delta G_{\text{syn}}^{\ddagger} = 7.9$ kcal/mol and $\Delta G_{\text{anti}}^{\ddagger} = 19.8$ kcal/mol). However, most interestingly, the order of reactivity is predicted to be different in the smaller models than in the larger models: that is, the *t*-BuSeOH/•OOME reaction is predicted to be *faster* than the corresponding *t*-BuSOH/•OOME reaction.⁴⁷ This is particularly surprising, given that the strength of the O–H bond in *t*-BuSeOH is predicted to be 12.6 kcal/mol *stronger* than the O–H bond in *t*-BuSOH!

The reactions of sulfenic acids with peroxy radicals have been described as taking place by proton-coupled electron transfer,^{15,31} facilitated by the overlap between orbitals based on the sulfenic acid sulfur atom and the inner oxygen atom of the peroxy radical—seen clearly in the three highest (doubly) occupied MOs shown in Figure 9—accounting for the preference for the syn TS in the formal H-atom transfer.⁴⁸ This description would appear to be appropriate for the reactions of selenenic acids with peroxy radicals as well, as the same interactions are evident in the corresponding MOs shown on the left in Figure 9. The lower barrier for the *t*-BuSeOH/•OOME reaction in comparison to that for *t*-BuSOH/•OOME via the low-energy syn pathway can therefore be understood on the basis of improved charge transfer between the larger, less electronegative selenium atom and the internal oxygen atom of the peroxy radical in comparison to the smaller, more electronegative sulfur atom. Indeed, bond order analysis of the structures in Figure 8 (and Figure 9)

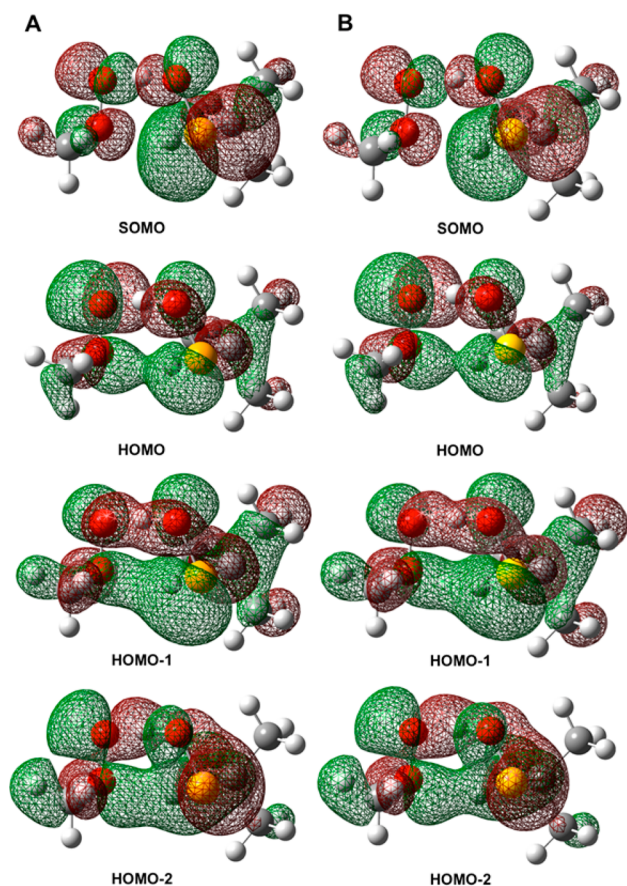


Figure 9. The four highest energy occupied molecular orbitals corresponding to the syn transition state structures for the reactions of *t*-BuSeOH (A) and *t*-BuSOH (B) with MeOO• obtained from the UB3LYP/CBSB7 step of the CBS-QB3 calculation.

reveals a much larger bonding interaction between the selenium atom and the internal oxygen atom of the peroxy radical in the selenenic acid syn TS (0.229) in comparison to the sulfur and corresponding oxygen atom in the sulfenic acid syn TS (0.180).⁴⁹

Since the high reactivity of selenenic acids toward peroxy radicals appears to be driven by charge transfer from the selenium to the internal oxygen atom of the peroxy radical, the barrier of the reaction should be highly dependent on the extent to which orbitals centered on these atoms overlap. To illustrate this point, we calculated the ΔG^\ddagger value for the reactions of *t*-BuSeOH with MeOO• as a function of the Se–O/O–O torsion angle in the TS structure. The results are shown in Figure 10, revealing a substantial dependence of the barrier height on the torsion angle: rising from ca. 8 kcal/mol to ca. 20 kcal/mol upon going from the syn structure to the orthogonal structure. We carried out analogous calculations for the reactions of *t*-BuSOH with MeOO•, which revealed a similar, but less severe, angular dependence; the barrier rises from ca. 10 kcal/mol to ca. 15 kcal/mol in the orthogonal structure (see also Figure 10).⁵⁰ Thus, while selenenic acids may be more reactive toward peroxy radicals than sulfenic acids at the “ideal” TS geometry, they become less reactive as the geometry is distorted to reduce the Se/O overlap in the TS. It seems reasonable to suggest that the triptycene moieties necessary to make the sulfenic and selenenic acids persistent and amenable to experimental study also make it difficult for them to achieve “ideal” TS geometries in reactions with peroxy

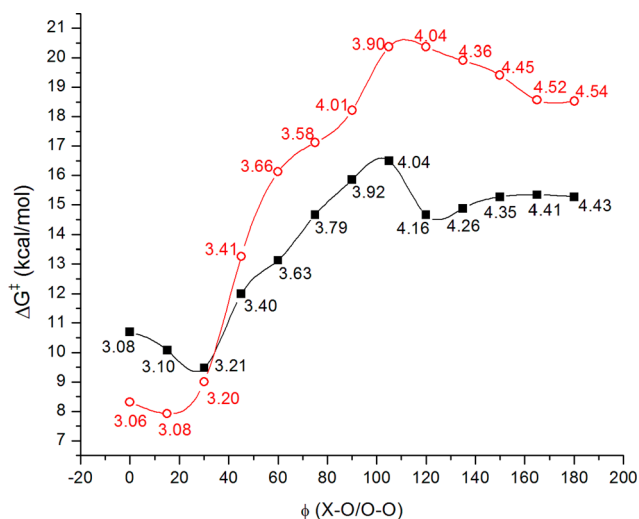


Figure 10. Dependence of the CBS-QB3-calculated ΔG^\ddagger values for the reactions of *t*-BuSeOH (red, open symbols) and *t*-BuSOH (black, closed symbols) with MeOO• on the Se–O/O–O and S–O/O–O torsion angles in the transition state structures, respectively. The points are labeled with the distance between the chalcogen atom and the inner oxygen atom of the peroxy radical in the corresponding structures.

radicals. Indeed, while the calculated TS structures in Figures 7 (full model) and 8 (smaller model) feature similar overall geometries, the distances between the chalcogen atom and the inner oxygen atom of the peroxy radical are significantly longer in the former in comparison to the latter (3.12 and 3.14 Å vs 3.01 and 3.00 Å), and the Se–O/O–O and S–O/O–O torsion angles have opened up to 17 and 20° from 9 and 10°, respectively,⁴³ diminishing overlap between the orbitals on the chalcogen atom and the internal oxygen atom of the peroxy radical.

The higher than expected reactivity of the persistent selenenic acid **2** toward peroxy radicals (relative to the persistent sulfenic acid **1**) is the strongest evidence to date for charge transfer/secondary orbital interactions in the reactions of good H-atom donors with peroxy radicals. While this has been suggested to be key to the reactions of ubiquitous radical-trapping antioxidants, such as phenols^{31,32} and diarylamines,^{33,34} as well as related compounds,^{15,35} it is yet to be firmly supported by experiment. Given that these reactions underlie the preservation of virtually all hydrocarbon materials (including us!), we trust the foregoing insights will help clarify structure–reactivity trends already established or yet to be uncovered with the design of new compounds.

CONCLUSIONS

A persistent selenenic acid bearing a triptycene moiety has been used to characterize the redox chemistry of selenenic acids for the first time. The strength of the O–H bond in the selenenic acid is ca. 81 kcal/mol, making it weaker than the corresponding O–H bond in a hydroperoxide (ca. 86 kcal/mol) but much stronger than in a sulfenic acid (ca. 70 kcal/mol).^{13,15} Insights from theoretical calculations indicate that the lack of any periodic trend in the BDEs is the result of lesser spin delocalization in the selenenyl radical relative to the sulfinyl radical, owing to the longer Se–O bond. As such, selenenic acids are unusual among the three (valence) isoelectronic species in that the O–H bond is stronger than the Se–H bond in the selenol (from which it is often derived).

This trend is in contrast with those established for sulfenic acids and hydroperoxides, which are characterized by significantly weaker bonds (by ca. 20 kcal/mol) to hydrogen than in the corresponding thiols and alcohols, respectively. These insights serve as a cautionary note on rationalizing the reactivity of selenium-containing compounds simply on the basis of their structural similarity to sulfur-containing compounds.

The kinetics of formal H-atom transfer reactions from the persistent selenenic acid were evaluated using peroxy radicals as a model oxidant, revealing very high reactivity ($k_{\text{inh}} = 1.7 \times 10^5 \text{ M}^{-1} \text{ s}^{-1}$) relative to the strength of the O–H bond. CBS-QB3 calculations on a model system wherein the triptycene is replaced with a *tert*-butyl group and a methylperoxy radical is used as the oxidant reveal that these reactions proceed with a negligible enthalpic barrier via a transition state stabilized greatly by interactions between orbitals with significant contributions from the selenium atom and the internal oxygen atom of the peroxy radical. The calculations also indicate that these interactions are highly sensitive to the transition state geometry; even small perturbations in the structure that diminish these interactions significantly increase ΔG^\ddagger and account for the lower observed reactivity of the hindered 9-triptyceneselenenic acid in comparison to that expected on the basis of the model calculations. These insights reveal the dramatic impact of small perturbations on the transition state geometries for formal H-atom transfer reactions facilitated by secondary orbital interactions (e.g., in proton-coupled electron transfer reactions). That is, steric arguments for the rationalization of reactivity trends must be considered carefully in light of the impact they have not only on potential approach trajectories of the reactants but also in their abilities to maximize secondary orbital overlap in the transition state.

The foregoing results indicate that unhindered selenenic acids are likely to be among the most reactive H-atom donors toward radical centers that have an adjacent high-lying electron pair, such as in peroxy or phenoxy radicals, which facilitate the reaction via interaction with orbitals centered on the selenium atom. As such, the formation of a selenenic acid either by oxidation of a selenol or by Cope elimination from a selenoxide may serve to convert a relatively poor H-atom donor into an excellent one and may present a complementary mechanism for the reducing activities of selenium compounds beyond the two-electron chemistry that is most commonly observed and/or assumed.

EXPERIMENTAL SECTION

Synthesis. Bis(2-phenethyl) Diselenide (3). Dry selenium powder (3.5 g, 44 mmol), sodium chips (1.06 g, 44 mmol), and naphthalene (0.57 g, 4.5 mmol) were stirred in dry THF (100 mL) under argon for 12 h. To the dark purple mixture was added 2-bromoethylbenzene (5.88 mL, 44 mmol) dropwise. The mixture was stirred for 1 h, during which the color changed to light orange. A tan salt was removed by filtration, and the filtrate was concentrated in vacuo. The resulting orange oil was loaded on a silica gel flash column and eluted first with hexanes and then with benzene to give an orange oil (7.77 g, 48% yield): $^1\text{H NMR}$ (400 MHz, CDCl_3) δ 3.03–3.07 (m, 4H), 3.14–3.18 (m, 4H), 7.20–7.24 (m, 6H), 7.29–7.33 (m, 4H); $^{13}\text{C NMR}$ (CDCl_3 , 300 MHz) δ 30.7, 37.5, 126.3, 128.4, 128.5, 140.7; HRMS (EI+) calculated for $\text{C}_{16}\text{H}_{18}\text{Se}_2$ 369.6739, observed 369.6735. The $^1\text{H NMR}$ spectrum is in good agreement with that presented in the literature;³⁶ the $^{13}\text{C NMR}$ spectrum has not been reported to date.

9-Triptycene Phenethyl Selenide (4). 9-Bromotriptycene¹³ (1.8 g, 5.4 mmol) was dissolved in dry benzene (100 mL), and dry methyl *tert*-butyl ether (70 mL), cooled to -18°C , and *n*-butyllithium (3.8 mL, 5.4 mmol) were added dropwise. Bis(phenethyl) diselenide (3;

2.1 g, 5.4 mmol) was suspended in a minimum amount of dry benzene and added slowly to the reaction mixture at 0°C . The reaction mixture was stirred at room temperature for 12 h, before it was quenched with water and extracted with ether. The organic phase was washed with brine and then dried over MgSO_4 , filtered, and concentrated in vacuo. The resulting oily yellow solid was loaded on a silica gel flash column and eluted with 5% dichloromethane in hexanes to yield an off-white solid which was recrystallized from benzene/ethanol (1.77 g, 75% yield): $^1\text{H NMR}$ (400 MHz, CDCl_3) δ 3.16–3.21 (m, 2H), 3.28–3.33 (m, 2H), 5.38 (s, 1H), 7.02–7.05 (m, 6H), 7.27–7.31 (m, 1H), 7.35–7.41 (m, 7H), 7.56–7.59 (m, 3H); $^{13}\text{C NMR}$ (400 MHz, CDCl_3) δ 25.7, 36.8, 54.1, 60.3, 123.4, 124.0, 125.0, 125.6, 126.6, 128.5, 128.6, 140.6, 145.1, 145.6; HRMS (EI+) calculated for $\text{C}_{28}\text{H}_{22}\text{Se}$ 438.0887, observed 438.0876.

9-Triptycene Phenethyl Selenoxide (5). A solution of 4 (94 mg, 0.21 mmol) in dry dichloromethane (18 mL) was cooled to -78°C . mCPBA (77%, 48 mg, 0.21 mmol) was added slowly in 5 mL of dry dichloromethane. The reaction mixture was worked up immediately by washing twice with 20 mL of cold 0.7 M aqueous KOH, followed by 20 mL of ice water, then 20 mL of cold brine. The organic phase was dried over MgSO_4 , filtered, and concentrated in vacuo at -78°C . A white solid was obtained (84 mg, 86% yield). The 9-triptycene phenethyl selenoxide was generally obtained as a mixture with 9-triptyceneselenenic acid and styrene due to Cope elimination in situ: $^1\text{H NMR}$ (300 MHz, CDCl_3) δ 3.47–3.64 (m, 2H), 3.83–3.93 (m, 1H), 4.00–4.09 (m, 1H), 5.37 (s, 1H), 7.02–7.05 (m, 6H), 7.28–7.37 (m, 9H) 7.93–8.02 (m, 1H), 8.31–8.39 (m, 1H); $^{13}\text{C NMR}$ (300 MHz, CDCl_3) δ 29.7, 30.5, 48.7, 68.1, 121.6, 123.0, 123.6, 125.3, 125.7, 127.1, 128.8, 129.0, 144.3, 145.7. No molecular ion could be observed by MS due to its ready fragmentation to the selenenic acid.

9-Triptyceneselenenic Acid (2). Selenoxide 5 was left under high vacuum for 2 weeks at room temperature: $^1\text{H NMR}$ (300 MHz, CDCl_3) δ 5.42 (s, 1H), 7.02–7.05 (m, 6H), 7.41–7.44 (m, 6H); $^{13}\text{C NMR}$ (300 MHz, CDCl_3) δ 54.1, 64.1, 123.0, 123.7, 125.3, 125.7, 144.3, 145.7; HRMS (ES-) calculated for $\text{C}_{20}\text{H}_{14}\text{OSe}$ 349.0132, observed 349.0104. The spectral characteristics are in good agreement with those presented in the literature.¹²

EPR Experiments. Spectra were recorded at 298 K by irradiating deoxygenated benzene solutions of 2 containing di-*tert*-butyl peroxide (10% v/v) with a 500W high-pressure Hg lamp in the spectrometer cavity. The measured g factor was corrected with respect to the known value of 2,2,6,6-tetramethylpiperidine-*N*-oxyl radical in benzene ($g = 2.0064$). Equilibration studies were performed by irradiating mixtures of 2 and 2,4,6-tri-*tert*-butylphenol¹⁹ in different ratios.^{18,33,37,38} The relative amount of the corresponding radicals was determined by fitting the experimental spectrum with computer simulations using WinESR software, developed by Prof. Marco Lucarini (Univ. Bologna), based on the Monte Carlo method.³⁷ Different irradiation intensities were compared to make sure that equilibrium was established. The equilibrium constant K was determined according to eq 5, which yielded ΔH for equilibration by eq 6 under the assumption that $\Delta S \approx 0$.^{33,37,38}

$$K = ([\text{TripSeOH}]/[\text{TTBP}]) \times ([\text{TTBP}^\bullet]/[\text{TripSeO}^\bullet]) \quad (5)$$

$$\Delta G = \Delta H - T\Delta S = -RT \ln K \quad (6)$$

Autoxidations. Rate constants (k_{inh}) for the reactions of 2 with peroxy radicals were determined by kinetic analysis of inhibited autoxidations of styrene (50% v/v) in air-saturated chlorobenzene or acetonitrile solution at 303 K.²⁴ The reaction was thermally initiated at constant rate R_i (determined experimentally, in the range $(2-9) \times 10^{-9} \text{ M s}^{-1}$) by the decomposition of 2,2'-azodiisobutyronitrile (AIBN, $(1-5) \times 10^{-2} \text{ M}$) and the oxygen consumption was monitored in a two-channel oxygen-uptake apparatus already described elsewhere.^{39,40} 2,2,5,7,8-Pentamethyl-6-chromanol (PMHC) was used as reference antioxidant.^{39,40} From the slope of the oxygen consumption during the inhibited period (R_{inh}), k_{inh} values were obtained by using eq 7, where R_0 is the rate of oxygen consumption in the absence of antioxidants, $2k_t$ is the bimolecular termination rate constant of styrene ($4.2 \times 10^7 \text{ M}^{-1} \text{ s}^{-1}$), and n is the stoichiometric coefficient of the antioxidant,

which was determined experimentally from the length of the inhibited period (τ) by eq 8.^{39,40} When the inhibited period was not clearly visible, kinetic data were confirmed by fitting the experimental traces with numerical simulations using Gepasi 3.0 software, as previously described.⁴¹

$$(R_0/R_{\text{inh}}) - (R_{\text{inh}}/R_0) = nk_{\text{inh}}[\text{AH}]/\sqrt{(2k_{\text{t}}R_1)} \quad (7)$$

$$n = \tau R_1/[\text{AH}] \quad (8)$$

Deuterium kinetic isotope effects were determined by comparing inhibited autoxidations recorded upon addition of 1% v/v H₂O or D₂O.^{39,40}

IR Measurements. Spectra of **1** and **2** were recorded at 298 K in a FT-IR spectrometer under a nitrogen atmosphere using a sealed KBr cell with an optical path of 0.5 mm. Solutions of the test compound (1–10 mM) in CCl₄ and in CCl₄/CH₃CN mixtures were analyzed in absorbance mode referenced to the blank spectrum of the corresponding solvent mixture. The integrated signal of the “free” O–H stretching mode at ca. 3530 cm⁻¹, obtained after manual baseline correction, was plotted vs the concentration of acetonitrile and fit to eq 9.

$$[\mathbf{1} \text{ or } \mathbf{2}]_{\text{free}} = [\mathbf{1} \text{ or } \mathbf{2}]_{\text{tot}}/(1 + K_{\text{sol}} \times [\text{Solv}]) \quad (9)$$

From the measured equilibrium constant K_{sol} , the corresponding α_2^{H} values were obtained by Abraham's eq 10,²⁷ using the revised value of $\beta_2^{\text{H}} = 0.39$ for acetonitrile.⁴⁴

$$\log(K_{\text{sol}}/M^{-1}) = 7.354\alpha_2^{\text{H}}\beta_2^{\text{H}} - 1.094 \quad (10)$$

Computations. All calculations were carried out using the Gaussian 09 quantum chemistry package⁵¹ using the CBS-QB3 complete basis set approach,²⁰ except for the calculated transition state structures shown in Figure 10, which were obtained using B3LYP and a 6-31+G(2d,2p) basis set including the dispersion-correcting potentials of DiLabio and Torres.³⁰ Wiberg bond order analysis⁵² was carried out using the AOMix software developed by Gorelsky.⁵³

■ ASSOCIATED CONTENT

● Supporting Information

NMR spectra of new compounds, representative voltammograms, Cartesian coordinates, and energies of stationary points determined by computation. This material is available free of charge via the Internet at <http://pubs.acs.org>.

■ AUTHOR INFORMATION

Corresponding Author

luca.valgimigli@unibo.it; dpratt@uottawa.ca

Notes

The authors declare no competing financial interest.

■ ACKNOWLEDGMENTS

We are grateful to the Natural Sciences and Engineering Research Council of Canada and the Canada Foundation for Innovation for grants to D.A.P. and the Italian MIUR, Rome (PRIN2011 2010PFLRJR (PROxi project)) for a grant to L.V. and R.A. The computations described herein were made possible by the High Performance Computing Virtual Laboratory. D.A.P. also acknowledges the support of the Canada Research Chairs program.

■ REFERENCES

- (1) Rappoport, Z. *The Chemistry of Organic Selenium and Tellurium Compounds*; Wiley: Hoboken, NJ, 2012.
- (2) Muges, G.; du Mont, W.-W.; Sies, H. *Chem. Rev.* **2001**, *101*, 2125–2180.

- (3) Goto, K.; Nagahama, M.; Mizushima, T.; Shimada, K.; Kawashima, T.; Okazaki, R. *Org. Lett.* **2001**, *3*, 3569–3572.
- (4) Jones, D. N.; Mundy, D.; Whitehouse, R. D. *J. Chem. Soc. D* **1970**, 86.
- (5) Sharpless, K. B.; Lauer, R. F. *J. Am. Chem. Soc.* **1973**, *95*, 2697–2699.
- (6) Reich, H. J.; Renga, J. M.; Reich, I. L. *J. Am. Chem. Soc.* **1975**, *97*, 5434–5447.
- (7) Flohe, L.; Gunzler, W. A.; Schock, H. H. *FEBS Lett.* **1973**, *32*, 132–134.
- (8) Rotruck, J. T.; Pope, A. L.; Ganther, H. E.; Swanson, A. B.; Hafeman, D. G.; Hoekstra, W. G. *Science* **1973**, *179*, 588–590.
- (9) Bhabak, K. P.; Muges, G. *Acc. Chem. Res.* **2010**, *43*, 1408–1419.
- (10) Reich, H. J.; Jasperse, C. P. *J. Org. Chem.* **1988**, *53*, 2389–2390.
- (11) Saiki, T.; Goto, K.; Okazaki, R. *Angew. Chem., Int. Ed. Engl.* **1997**, *36*, 2223–2224.
- (12) Ishii, A.; Matsubayashi, S.; Takahashi, T.; Nakayama, J. *J. Org. Chem.* **1999**, *64*, 1084–1085.
- (13) McGrath, A. J.; Garrett, G. E.; Valgimigli, L.; Pratt, D. A. *J. Am. Chem. Soc.* **2010**, *132*, 16759–16761.
- (14) Amorati, R.; Lynett, P. T.; Valgimigli, L.; Pratt, D. A. *Chem. Eur. J.* **2012**, *18*, 6370–6379.
- (15) Vaidya, V.; Ingold, K. U.; Pratt, D. A. *Angew. Chem., Int. Ed.* **2009**, *48*, 157–160.
- (16) Lynett, P. T.; Butts, K.; Vaidya, V.; Garrett, G. E.; Pratt, D. A. *Org. Biomol. Chem.* **2011**, *9*, 3320–3330.
- (17) Paulsen, C. E.; Carroll, K. S. *Chem. Rev.* **2013**, *113*, 4633–4679.
- (18) Lucarini, M.; Pedulli, G. F.; Cipollone, M. *J. Org. Chem.* **1994**, *59*, 5063–5070.
- (19) Mulder, P.; Korth, H.-G.; Pratt, D. A.; DiLabio, G. A.; Valgimigli, L.; Pedulli, G. F.; Ingold, K. U. *J. Phys. Chem. A* **2005**, *109*, 2647–2655.
- (20) Montgomery, J. A.; Frisch, M. J.; Ochterski, J. W.; Petersson, G. A. *J. Chem. Phys.* **1999**, *110*, 2822.
- (21) Gibson, S. T. *J. Chem. Phys.* **1986**, *85*, 4815–4824.
- (22) Leeck, D. T.; Li, R.; Chyall, L. J.; Kenttämaa, H. I. *J. Phys. Chem.* **1996**, *100*, 6608–6611.
- (23) Janousek, B. K.; Reed, K. J.; Brauman, J. I. *J. Am. Chem. Soc.* **1980**, *102*, 3125–3129.
- (24) Burton, G. W.; Doba, T.; Gabe, E.; Hughes, L.; Lee, F. L.; Prasad, L.; Ingold, K. U. *J. Am. Chem. Soc.* **1985**, *107*, 7053–7065.
- (25) Snelgrove, D. W.; Lusztyk, J.; Banks, J. T.; Mulder, P.; Ingold, K. U. *J. Am. Chem. Soc.* **2001**, *123*, 469–477.
- (26) Litwinienko, G.; Ingold, K. U. *Acc. Chem. Res.* **2007**, *40*, 222–230.
- (27) Abraham, M. H.; Grellier, P. L.; Prior, D. V.; Morris, J. J.; Taylor, P. J. *J. Chem. Soc., Perkin Trans. 2* **1990**, 521.
- (28) Valgimigli, L.; Pratt, D. A. In *Encyclopedia of Radicals in Chemistry, Biology and Materials*; Wiley: Chichester, U.K., 2012; Vol. 3, pp 1623–1677.
- (29) Ishii, A.; Komiya, K.; Nakayama, J. *J. Am. Chem. Soc.* **1996**, *118*, 12836–12837.
- (30) Torres, E.; DiLabio, G. A. *J. Phys. Chem. Lett.* **2012**, *3*, 1738–1744.
- (31) DiLabio, G. A.; Johnson, E. R. *J. Am. Chem. Soc.* **2007**, *129*, 6199–6203.
- (32) Valgimigli, L.; Amorati, R.; Petrucci, S.; Pedulli, G. F.; Hu, D.; Hanthorn, J. J.; Pratt, D. A. *Angew. Chem., Int. Ed.* **2009**, *48*, 8348–8351.
- (33) Hanthorn, J. J.; Valgimigli, L.; Pratt, D. A. *J. Am. Chem. Soc.* **2012**, *134*, 8306–8309.
- (34) Hanthorn, J. J.; Amorati, R.; Valgimigli, L.; Pratt, D. A. *J. Org. Chem.* **2012**, *77*, 6895–6907.
- (35) Amorati, R.; Pedulli, G. F.; Pratt, D. A.; Valgimigli, L. *Chem. Commun.* **2010**, 46, 5139.
- (36) Thompson, D. P.; Boudjouk, P. *J. Org. Chem.* **1988**, *53*, 2109–2112.
- (37) Lucarini, M.; Pedrielli, P.; Pedulli, G. F.; Cabiddu, S.; Fattuoni, C. *J. Org. Chem.* **1996**, *61*, 9259–9263.

(38) Shanks, D.; Amorati, R.; Fumo, M. G.; Pedulli, G. F.; Valgimigli, L.; Engman, L. *J. Org. Chem.* **2006**, *71*, 1033–1038.

(39) Lucarini, M.; Pedulli, G. F.; Valgimigli, L.; Amorati, R.; Minisci, F. *J. Org. Chem.* **2001**, *66*, 5456–5462.

(40) Amorati, R.; Pedulli, G. F.; Valgimigli, L. *Org. Biomol. Chem.* **2011**, *9*, 3792–3800.

(41) Valgimigli, L.; Amorati, R.; Fumo, M. G.; DiLabio, G. A.; Pedulli, G. F.; Ingold, K. U.; Pratt, D. A. *J. Org. Chem.* **2008**, *73*, 1830–1841.

(42) The increased O–H BDE in **1** in comparison to *t*-BuSOH is likely the result of the three sp² carbons bound to the quaternary carbon in the former being more inductively withdrawing than the sp³ carbons in the latter, stabilizing the starting material and destabilizing the radical from **1** relative to *t*-BuSOH.

(43) The CCSD(T), MP2, and MP4 steps of the CBS-QB3 calculation each predict a spin distribution of ca. 0.2/0.8 (Se/O) in the selenenyl radical and ca. 0.4/0.6 (S/O) in the sulfinyl radical, whereas B3LYP predicts roughly 0.5/0.5 in both. The inclusion of effective core potentials in these calculations did not change the spin distributions to any significant extent.

(44) Valgimigli, L.; Bartolomei, D.; Amorati, R.; Haidasz, E.; Hanthorn, J. J.; Nara, S. J.; Brinkhorst, J.; Pratt, D. A. *Beilstein J. Org. Chem.* **2013**, *9*, 2781–2792.

(45) Ingold's equation refers to the KSE in pure solvents, while kinetics were measured in 50% v/v styrene/solvent mixtures.

(46) This is unsurprising, given that the calculations are of isolated molecules and the experiments were carried out in chlorobenzene, which would slow the reaction slightly due to H bonding; see refs 25 and 26.

(47) It must be pointed out that the DCP-B3LYP approach used to calculate the TS structures for the reactions of **1** and **2** with styrylperoxyl radicals also predicts a lower free energy barrier (by 1.2 kcal/mol) for the *t*-BuSeOH/[•]OOME reaction in comparison to the *t*-BuSOH/[•]OOME reaction, in good agreement with the CBS-QB3 calculations.

(48) This can also be described simply as an H-atom transfer reaction facilitated by a secondary orbital interaction, which lowers the energy of the syn TS relative to the anti TS. For a related example, see: Hu, D.; Pratt, D. A. *Chem. Commun.* **2010**, *46*, 3711–3713.

(49) In contrast, the anti TS structures have essentially the same bond order between the chalcogen atom and the internal oxygen atom of the peroxy radical (S/O, 0.096; Se/O, 0.101).

(50) The optimal TS structure is calculated for a Se–O/O–O or S–O/O–O torsion angle of roughly 20° due to the orbital overlap between the chalcogen atom and inner peroxy atom in the HOMO, which is impossible at a torsion angle of 0°.

(51) Frisch, M. J.; Trucks, G. W.; Schlegel, H. B.; Scuseria, G. E.; Robb, M. A.; Cheeseman, J. R.; Scalmani, G.; Barone, V.; Mennucci, B.; Petersson, G. A.; Nakatsuji, H.; Caricato, M.; Li, X.; Hratchian, H. P.; Izmaylov, A. F.; Bloino, J.; Zheng, G.; Sonnenberg, J. L.; Hada, M.; Ehara, M.; Toyota, K.; Fukuda, R.; Hasegawa, J.; Ishida, M.; Nakajima, T.; Honda, Y.; Kitao, O.; Nakai, H.; Vreven, T.; Montgomery, J. A., Jr.; Peralta, J. E.; Ogliaro, F.; Bearpark, M.; Heyd, J. J.; Brothers, E.; Kudin, K. N.; Staroverov, V. N.; Keith, T.; Kobayashi, R.; Normand, J.; Raghavachari, K.; Rendell, A.; Burant, J. C.; Iyengar, S. S.; Tomasi, J.; Cossi, M.; Rega, N.; Millam, J. M.; Klene, M.; Knox, J. E.; Cross, J. B.; Bakken, V.; Adamo, C.; Jaramillo, J.; Gomperts, R.; Stratmann, R. E.; Yazyev, O.; Austin, A. J.; Cammi, R.; Pomelli, C.; Ochterski, J. W.; Martin, R. L.; Morokuma, K.; Zakrzewski, V. G.; Voth, G. A.; Salvador, P.; Dannenberg, J. J.; Dapprich, S.; Daniels, A. D.; Farkas, O.; Foresman, J. B.; Ortiz, J. V.; Cioslowski, J.; Fox, D. J. *Gaussian 09, revision B.01*; Gaussian, Inc., Wallingford, CT, 2009.

(52) Mayer, I. *Chem. Phys. Lett.* **1983**, *97*, 270–274. Wiberg, K. B. *Tetrahedron* **1968**, *24*, 1083–1096.

(53) Gorelsky, S. I. *AOMix: Program for Molecular Orbital Analysis, version 6.82*, 2013; <http://www.sg-chem.net/>. Gorelsky, S. I.; Lever, A. B. P. *J. Organomet. Chem.* **2001**, *635*, 187–196.